Induction Period of $CaCO_3$ Interpreted by the Smoluchowski's Coagulation Theory

C. Y. Tai, W. C. Chien, and J. P. Hsu
Dept. of Chemical Engineering, National Taiwan University, Taipei, Taiwan, 10617

DOI 10.1002/aic.10304
Published online in Wiley InterScience (www.interscience.wiley.com).

Smoluchowski's coagulation theory is adopted to estimate the induction period for the formation of the critical nuclei of $CaCO_3$ in a supersaturated $CaCl_2$-Na_2CO_3 aqueous solution. The effects of the presence of impurity and crystal seeds, degree of supersaturation and operating temperature on the induction period are discussed. The association coefficient between two clusters is found to depend on both the degree of supersaturation and the temperature. The estimated activation energy for the association between two clusters is about 200 J/mol, which implies that the association between two clusters is of physical nature. It is found that the increase in the induction period with the presence of Mg^{2+} may be caused by an increase in the solid-liquid interfacial energy, and a decrease in the association coefficient. Due to van der Waals attraction, the addition of crystal seeds increases the concentration of clusters near seed surface, and, thus, yields a shorter induction period. © 2005 American Institute of Chemical Engineers *AIChE J,* 51: 480–486, 2005
Keywords: Calcium carbonate, induction period, effect of operating variables, Smoluchowski's coagulation theory, association coefficient

Introduction

The classical theory of homogeneous nucleation indicates that when the solution is supersaturated the monomers in solution start to coagulate and then to form clusters. The existence of clusters in a supersaturated solution has been justified experimentally.[1-3] If the size of a cluster exceeds a critical size, a nucleus is formed, and the subsequent growth of nucleus leads to a crystal. The time interval between the onset of supersaturation and the formation of a cluster of critical size is defined as the induction period t_{ind}. Many methods, including conductivity,[4,5] intensity of transmitted or scattered light,[6-8] heat released,[9,10] activity of precipitated ions[11] and pH of solution,[12] have been applied for the determination of induction period. The results show that the induction period decreases with an increase in supersaturation, temperature, and agitation speed. The presence of impurity in solution prolongs the induction period. On the other hand, the addition of seed in solution reduces the induction period.

In theoretical, Söhnel and Mullin[13] have analyzed the induction period resulting from various nucleation and growth mechanisms for the case of unseeded precipitation. From the dependence of the induction period on solution supersaturation, it is possible to deduce whether the new phase appearance is governed either by nucleation (or nucleation followed by growth) or by growth alone. Verdoes et al.[11] derived a general expression of induction period by using a combined analysis of the induction period in both seeded and unseeded precipitation. These expressions are used for finding the dependence of induction period on the supersaturation for different nucleation and crystal growth mechanisms. Qian and Botsaris[14] proposed a model, which takes the interaction force between cluster and seed surface into account, to calculate the induction period and nucleation rate for interpreting the catastrophic secondary nucleation. In a recent study, Chien et al.[15] derived a kinetic model to estimate the induction period of $CaCO_3$ in a supersaturated $CaCl_2$-Na_2CO_3 aqueous solution. For simplicity, it is assumed that the size of a cluster increases geometrically, that is, the number of elementary entities contained in a cluster has

Correspondence concerning this article should be addressed to C. Y. Tai at cytai@ntu.edu.tw.

a value of 2^k, where k is a positive integer. Apparently, this model is an idealized one since the aggregation of clusters of various sizes may lead to a larger cluster of arbitrary size.

In this work, the induction period of the precipitation of $CaCO_3$ is calculated based on Smoluchowski's coagulation theory, which yields the temporal variation of cluster size distribution. This is an extension of our previous analysis in that a more realistic and rigorous kinetic mechanism is considered. The effects of the presence of impurity and seed crystals, degree of supersaturation, and operating temperature on the induction period are also discussed.

Theoretical

Suppose that the collision of two clusters yields a larger cluster containing the sum of the entities in each, and the breakup of a large cluster yields two smaller ones. Then, the temporal variation in cluster size distribution can be described by Smoluchowski's coagulation theory[16]

$$\frac{dC_n}{dt} = \frac{1}{2}\sum_{k=1}^{n-1}\left[a_{n-k,k}C_{n-k}C_k - b_{n-k,k}C_n\right] - \sum_{k=1}^{\infty}\left[a_{nk}C_nC_k - b_{nk}C_{n+k}\right] \quad (1)$$

where C_n is the concentration of clusters of size n (n-mer), a_{ij} is the association coefficient between clusters of sizes i (i-mer) and j (j-mer), b_{ij} is the dissociation coefficient of clusters of size (i+j), and t denotes time. Here, a_{ij} measures the rate of formation of clusters of size (i+j) through association of clusters of sizes i and j, and b_{ij} determines the rate of formation of clusters of size i (or j) through breakup of clusters of size (i+j). If $b_{ij}=0$, it can be shown that Eq.1 can be solved analytically for the following three special cases [17]

$$\text{Case 1: } a_{ij} = K_1 \quad (2a)$$

$$\text{Case 2: } a_{ij} = K_2(i+j) \quad (2b)$$

$$\text{Case 3: } a_{ij} = K_3 ij \quad (2c)$$

In these expressions K_1, K_2, and K_3 are constants. Equation 2a implies that the rate of formation of a cluster is independent of the sizes of its precursors. Equation 2b suggests that the rate of formation of a cluster is proportional to the sum of the sizes of its precursors, and Eq. 2c states that the rate of formation of a cluster is proportional to the product of the sizes of its precursors. The temporal variation in mean cluster size $\bar{n}$, can be derived according to Eqs. 2a–2c [17]

$$\text{Case 1: } \bar{n} = 1 + \frac{K_1 C_o t}{2} \quad (3a)$$

$$\text{Case 2: } \bar{n} = \exp(K_2 C_o t) \quad (3b)$$

$$\text{Case 3: } \bar{n} = \frac{2}{2 - K_3 C_o t} \quad (3c)$$

where C_o denotes the initial concentration of monomers.

According to the classical theory of homogeneous nucleation, when a solution is supersaturated the monomers in solution start to coagulate and then form clusters. If the size of a cluster exceeds a critical size g_c, a critical nucleus is born, and its subsequent growth leads to a crystal. The critical cluster size can be estimated by employing the thermodynamics arguments,[18] and was derived by Qian and Botsaris[14]

$$g_c = \frac{32\pi V_m^2 \delta^3}{3(kT \ln S_a)^3} \quad (4)$$

In this expression, V_m is the volume of a monomer, δ is the interfacial tension of crystal, k is the Boltzmann constant, T is the absolute temperature, and S_a is the degree of supersaturation, which can be evaluated by

$$S_a = \frac{C_{CaCO_3}\gamma_{\pm}}{C_{CaCO_3 eq}\gamma_{\pm eq}} \quad (5)$$

where C_{CaCO_3} is the initial concentration of $CaCO_3$, $C_{CaCO_3 eq}$ is the equilibrium concentration of $CaCO_3$ in an aqueous NaCl solution, which can be found in the literature,[19,20] and $\gamma_{\pm}$ and $\gamma_{\pm eq}$ are the mean activity coefficient and equilibrium mean activity coefficient, respectively, which can be estimated by Bromley correlation.[21]

We assume that when the mean cluster size in a solution reaches the critical cluster size the primary nucleation occurs spontaneously. The time at which $\bar{n}$ reaches to g_c is defined as the induction period t_{ind}. Let $\bar{n}=g_c$ and $t=t_{ind}$ in Eqs. 3a–3c, and solve the resultant expressions for t_{ind}, we obtain

$$\text{Case 1: } t_{ind} = \frac{2}{K_1 C_o}(g_c - 1) \quad (6a)$$

$$\text{Case 2: } t_{ind} = \frac{1}{K_2 C_o}\ln g_c \quad (6b)$$

$$\text{Case 3: } t_{ind} = \frac{2}{K_3 C_o}\left(1 - \frac{1}{g_c}\right) \quad (6c)$$

These expressions, together with Eqs. 4 and 5, provide the formulae for the calculation of the induction period.

When impurities are present in the solution, they may affect crystal growth. Consider, for example, magnesium ions as the impurities, the interfacial tension of $CaCO_3$, δ, varies accordingly, and our experimental results reveal that[22]

$$\delta = 2028.4 \times [Mg^{2+}] + 68.4 \quad (7)$$

Substituting this expression into Eq. 4 gives the critical nuclei size when Mg^{2+} is present in the liquid phase. Then the induction period can be estimated using Eqs. 6a–6c for various cases.

Experimental evidence reveals that the introduction of crystal seeds will accelerate the rate of crystal growth. Due to van der Waals attractive force, the concentration of clusters near the surface of a seed is higher than that in the bulk liquid phase, and, therefore, the rate of association between clusters is ac-

celerated. It can be shown that the concentration of spherical monomers of radius r_1 at a distance d from seed surface C'_o, is[14]

$$C'_o = C_o \exp\left(\frac{A}{6kT}\frac{r_1}{d}\right) \tag{8}$$

where C_o is the bulk concentration of monomers, and A is the Hamaker constant, which is about 1.61×10^{-20} J for $CaCO_3$.[23] The most proper value of d is 3.2×10^{-10} m for $CaCO_3$.[22] The induction period for the case, when crystal seeds are present, can be estimated by replacing C_o with C'_0 in Eqs. 6a–6c.

Results and Discussion

This theoretical model is fitted to the experimental data of $CaCO_3$ in a supersaturated $CaCl_2$-Na_2CO_3-H_2O solution. The experimental data used in this study have been reported in a previous study.[24] The applicability of Eqs. 6a–6c is first examined to determine the association mechanism. The result obtained is then applied to interpret the effects of Mg^{2+} impurity, seed crystals, degree of supersaturation, and operating temperature on the induction period.

Estimation of association coefficient

To calculate the induction period, based on Eqs. 6a–6c, the following values are used: $k=1.38 \times 10^{-23}$ J/K, and $V_m=6.13 \times 10^{-29}$ m^3/molecule, which is calculated by $M_w/\rho N$ using $M_w=0.1$ kg/mol, $\rho=2710$ kg/m^3 and $N=6.02 \times 10^{23}$ molecules/mol. The average value of interfacial tension, δ, in the absence of impurities is about 68.4 mJ/m^2 over the supersaturation range, $3< S_a <10$,[22] and this value is used in all the calculations except that when impurities are present. Then, the most proper values of association coefficient K_1, K_2, and K_3 in Eqs. 6a, 6b, and 6c, respectively, are further estimated by fitting the experimental data of induction period.

The theoretical values of t_{ind} calculated from three different association mechanisms and coefficients are summarized in Table 1. Examining Table 1, we notice that Eq. 6a fits best among the three. The determination of best mechanism is based on the total absolute deviation, ε, between the theoretical and experimental induction periods. The ε is defined as $\sum |t_{ind,\exp} - t_{ind,the}|/t_{ind,\exp}$. The values of ε obtained from different mechanisms and association coefficients are also listed in Table 1. The values of ε show that mechanism based on Eq. 6a with constant $K_1=2 \times 10^{-18}$ gives the smallest value of $\varepsilon = 3.02$. Therefore, the theoretical curve fitted by the theoretical points of Eq. 6a at $K_1=2 \times 10^{-18}$ are most close to the experimental points. Furthermore, analysis of experimental data is based on this model, which means that the association coefficient is independent of cluster size. The results indicate the decrease in the induction period at higher degree of supersaturation, which gives a smaller critical nuclei size and a larger initial concentration of clusters for their association. Figure 1 illustrates the theoretical induction period calculated from Eq. 6a. The curves in this figure were fitted using theoretical values. The experimental data are also shown in the figure for comparison. The association coefficients used in Figure 1 to calculate the induction period are $K_1=1 \times 10^{-18}$, 2×10^{-18}, and 4×10^{-18}.

Effect of temperature

Figure 2 shows the theoretical results based on Eq. 6a, and the experimental data for the induction period as a function of supersaturation at three different levels of temperature. This figure suggests that K_1 depends on the temperature. As mentioned in the section of supersaturation effect, the best values of K_1, based on the total absolute deviation, ε, must be found before calculating the theoretical induction period from Eq. 6a. It is found that smallest value of ε calculated at different temperature is $\varepsilon=1.89$ for $K_1=1 \times 10^{-18}$ at T=288K, $\varepsilon=1.01$ for $K_1=2 \times 10^{-18}$ at T=298K, and $\varepsilon=4.18$ for $K_1=3 \times 10^{-18}$ at T=308K. Therefore, the most proper values of K_1 for calculating induction period at different temperature are 1×10^{-18}, 2×10^{-18}, 3×10^{-18} for T=288k, 298K, and 308K, respectively. The results show that the calculated induction periods are in a good agreement with the experimental values. The decrease in the induction period at a higher temperature could be interpreted by a change in association coefficient, which implies a higher association rate between two solute clusters at higher temperature. We suppose that the dependence of the association coefficient K_1 on the temperature takes the Arrhenius form

$$K_1 = K_o \exp\left(-\frac{E_a}{RT}\right) \tag{9}$$

where E_a denotes the activation energy for the association of clusters, and K_o is a constant. According to Eq. 9, a plot of $\ln K_1$ against 1/T should yield a straight line with a slope of $-E_a/R$. The linear relation between $\ln K_1$ and 1/T is justified by Figure 3; the slope of the straight line is -24.05, and the activation energy for the association of clusters is about 200 J/mol. This result implies that the association between two clusters is of physical nature.

Effect of impurity

Table 2 shows the experimental data of induction period (column 3) reported in the literature[5, 24] at different levels of initial concentrations of $CaCl_2$ and Na_2CO_3 (column 1), and various molar concentration ratios of magnesium to calcium ion (column 2). In a narrow supersaturation region the interfacial tension is independent of supersaturation and can be expressed as a function of concentration of magnesium ions, that is, Eq. 7.[22] The calculated δ under different Mg^{2+} concentrations are presented in column 4. Then the values of δ are substituted into Eq. 4 to obtain the critical nuclei sizes g_c summarized in column 5. A further substitution of $t_{ind,\exp}$ and g_c into Eq. 6a, the corresponding values of K_1 are obtained and they are shown in column 6. As can be seen in Table 2, K_1 decreases with the increase in $[Mg^{2+}]/[Ca^{2+}]$ at each level of $CaCl_2$ (or Na_2CO_3) concentration. Figure 4 summarizes the variation of K_1 as a function of $[Mg^{2+}]/[Ca^{2+}]$. A regression analysis yields the following empirical equation with a correlation coefficient of 0.89

$$K_1 = 1.238 \times 10^{-18}\left(1.322 - \frac{[Mg^{2+}]}{[Ca^{2+}]}\right) \tag{10}$$

Table 1. A Comparison of the Association Coefficient at 298 K and Calculated ε for Three Different Association Mechanisms

S_a [-]	$t_{ind,exp}$ [s]	$t_{ind,the}$ [s] Based on Eq. (6a) $K_1 = 1 \times 10^{-18}$	Based on Eq. (6a) $K_1 = 2 \times 10^{-18}$	Based on Eq. (6a) $K_1 = 4 \times 10^{-18}$	Based on Eq. (6b) $K_2 = 1 \times 10^{-20}$	Based on Eq. (6b) $K_2 = 1 \times 10^{-19}$	Based on Eq. (6b) $K_2 = 1 \times 10^{-18}$	Based on Eq. (6c) $K_3 = 1 \times 10^{-20}$	Based on Eq. (6c) $K_3 = 1 \times 10^{-19}$	Based on Eq. (6c) $K_3 = 1 \times 10^{-18}$
4.37	550	594.69	297.34	148.67	862.62	86.26	8.63	330.38	33.04	3.30
5.06	202	294.57	147.29	73.64	542.40	54.24	5.42	219.83	21.98	2.20
5.79	94	172.76	86.38	43.19	386.54	38.65	3.87	164.53	16.45	1.65
6.41	78	118.27	59.14	29.57	298.99	29.90	2.99	131.41	13.14	1.31
6.90	45	87.49	43.74	21.87	242.64	24.26	2.43	109.36	10.94	1.09
7.37	36	67.39	33.70	16.85	202.97	20.30	2.03	93.60	9.36	0.94
7.88	24	53.99	26.99	13.50	173.99	17.40	1.74	81.80	8.18	0.82
8.41	13	45.77	22.89	11.44	152.94	15.29	1.53	72.66	7.27	0.73
8.81	28	35.14	17.57	8.78	128.59	12.86	1.29	62.75	6.27	0.63
9.41	18	29.14	14.57	7.29	114.58	11.46	1.15	57.14	5.71	0.57
10.0	8	22.81	11.40	5.70	95.46	9.55	0.95	48.53	4.85	0.49
*ε		10.21	3.02	5.70	54.13	4.88	10.35	20.02	7.98	10.70

*$\varepsilon = \Sigma\ |t_{ind,exp} - t_{ind,the}|/t_{ind,exp}$.

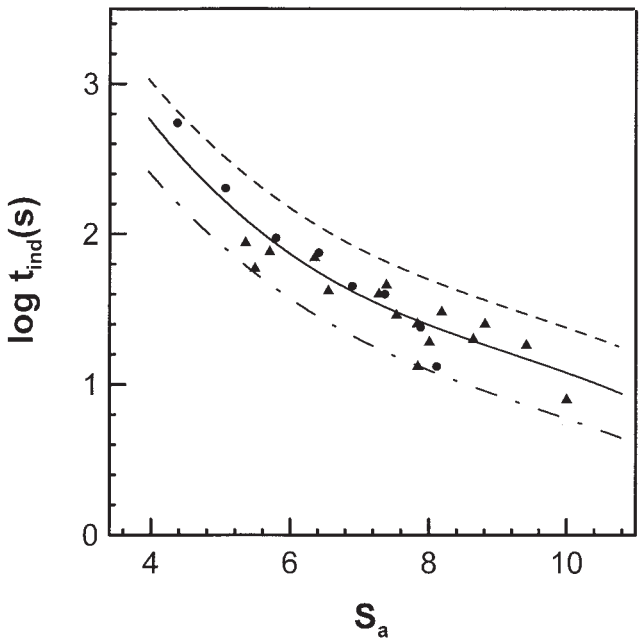

Figure 1. Variation in the induction period calculated by Eq.6a as a function of supersaturation at three different values of association coefficient.

Discrete points represent experimental data. ▲ : Söhnel and Mullin[5], ● : Chien et al.[15]. - - : $K_1 = 1 \times 10^{-18}$, — : $K_1 = 2 \times 10^{-18}$, — · — $K_1 = 4 \times 10^{-18}$.

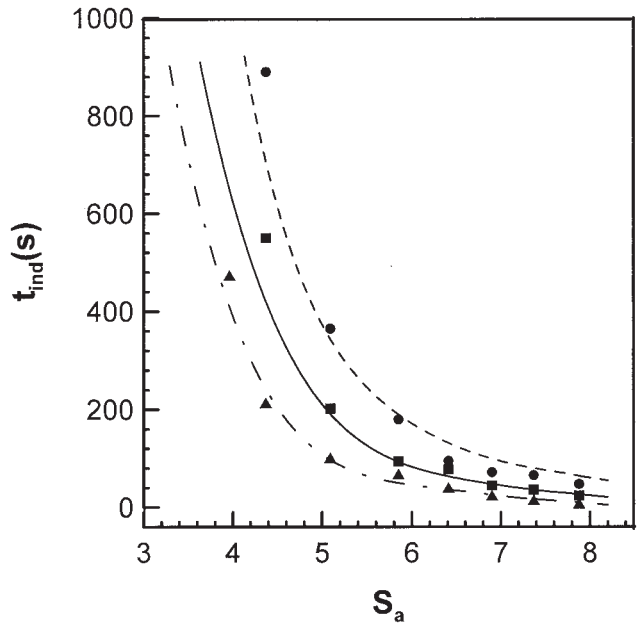

Figure 2. Variation in the induction period as a function of supersaturation at various solution temperatures.

Discrete points represent experimental data and the curves represent theoretical values predicted by this model. ● : T = 288 K, ■ : T = 298 K, ▲ : T = 308 K.[24] - - : $K_1 = 1 \times 10^{-18}$ for 288 K, — : $K_1 = 2 \times 10^{-18}$ for 298 K, — · — : $K_1 = 3 \times 10^{-18}$ for 308 K.

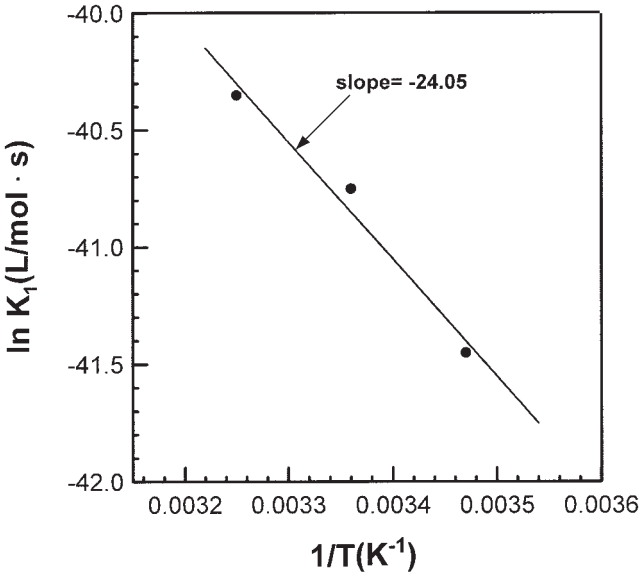

Figure 3. Variation of $\ln K_1$ as a function of 1/T for case 1.

Figure 5 illustrates the variation of the induction period as a function of the concentration ratio $[Mg^{2+}]/[Ca^{2+}]$ at various initial concentrations of $CaCl_2$ or Na_2CO_3, using the experimental data reported by Söhnel and Mullin,[5] and Tai and Chien,[24] and the theoretical values predicted by this model. The theoretical values are calculated by Eq. 6a in which K_1 is calculated from Eq. 10, and g_c is estimated by substituting Eq.

Table 2. The Theoretical Value of K_1 is Calculated by Substituting t_{ind} (column 3) and its Corresponding Value of g_c (column 5) into Eq. (6a) for Different Levels of Initial Reagent Concentration and Concentration Ratio of Mg^{2+} to Ca^{2+} at 25°C

$[CaCl_2] = [Na_2CO_3]$ [mol/L]	$\frac{[Mg^{2+}]}{[Ca^{2+}]}$ [-]	$t_{ind,exp}$ [s]	δ [mJ/m^2]	g_c [-]	K_1 ($\times 10^{19}$) [L/mol · s]
0.0015*	0.2	210	69.0	139	14.5
	0.4	250	69.6	143	12.6
	0.6	345	70.2	147	9.37
	0.8	375	70.8	151	8.86
	1.0	510	71.4	154	6.65
0.0025*	0.2	90	69.4	94	13.8
	0.4	145	70.4	98	8.89
	0.6	180	71.4	103	7.53
	0.8	240	72.5	107	5.87
	1.0	360	73.5	112	4.10
0.0035*	0.2	54	69.8	77	13.4
	0.4	70	71.2	82	11.0
	0.6	96	72.7	87	8.50
	0.8	150	74.1	92	5.76
	1.0	225	75.5	98	4.09
0.0040*	0.2	36	70.0	70	15.9
	0.4	54	71.6	75	11.4
	0.6	84	73.3	81	7.91
	0.8	132	74.9	86	5.35
	1.0	210	76.5	92	3.60
0.0045**	0.2	14	70.2	65	33.8
	0.4	40	72.1	71	12.9
	0.6	70	73.9	76	7.91
	0.9	140	76.6	85	4.43

* Experimental data of Tai and Chien.[24]
**Experimental data of Söhnel and Mullin.[5]

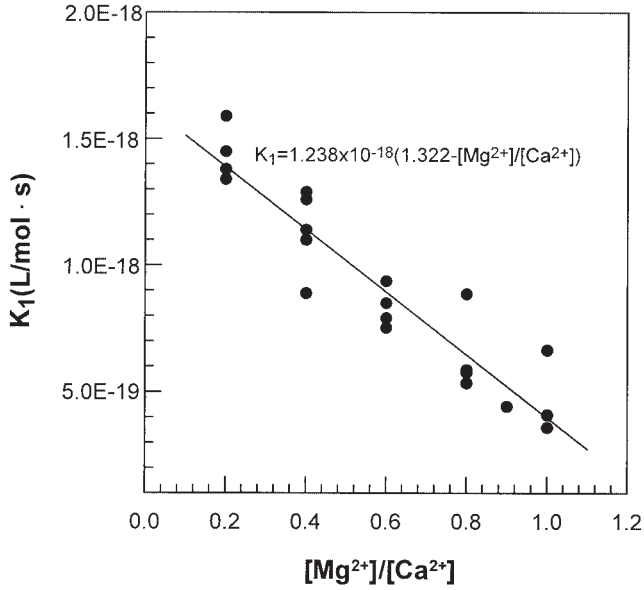

Figure 4. Variation in the association coefficient K_1 as a function of the molar concentration ratio $[Mg^{2+}]/[Ca^{2+}]$ at T=298 K.

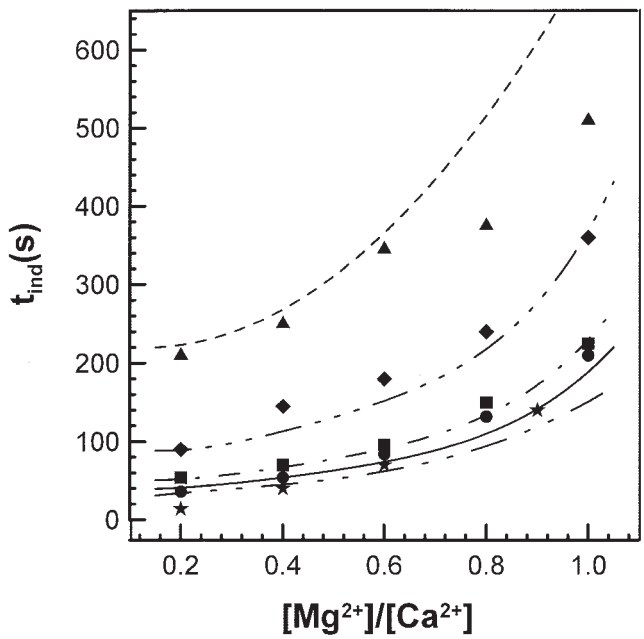

Figure 5. Variation of the induction period as a function of the molar concentration ratio $[Mg^{2+}]/[Ca^{2+}]$ at various concentrations of $CaCl_2$ (or Na_2CO_3).

Discrete points represent experimental data, and the curves represent theoretical values predicted by this model. ▲ : $[CaCl_2] = [Na_2CO_3] = 0.0015$ mol/L.[24] ◆ : $[CaCl_2] = [Na_2CO_3] = 0.0025$ mol/L.[24] ■ : $[CaCl_2] = [Na_2CO_3] = 0.0035$ mol/L.[24] ● : $[CaCl_2] = [Na_2CO_3] = 0.0040$ mol/L.[24] ★ : $[CaCl_2] = [Na_2CO_3] = 0.0045$ mol/L.[5] - - - : $[CaCl_2] = [Na_2CO_3] = 0.0015$ mol/L. — — — — : $[CaCl_2] = [Na_2CO_3] = 0.0025$ mol/L. — – — : $[CaCl_2] = [Na_2CO_3] = 0.0035$ mol/L. — : $[CaCl_2] = [Na_2CO_3] = 0.0040$ mol/L. — – – — : $[CaCl_2] = [Na_2CO_3] = 0.0045$ mol/L.

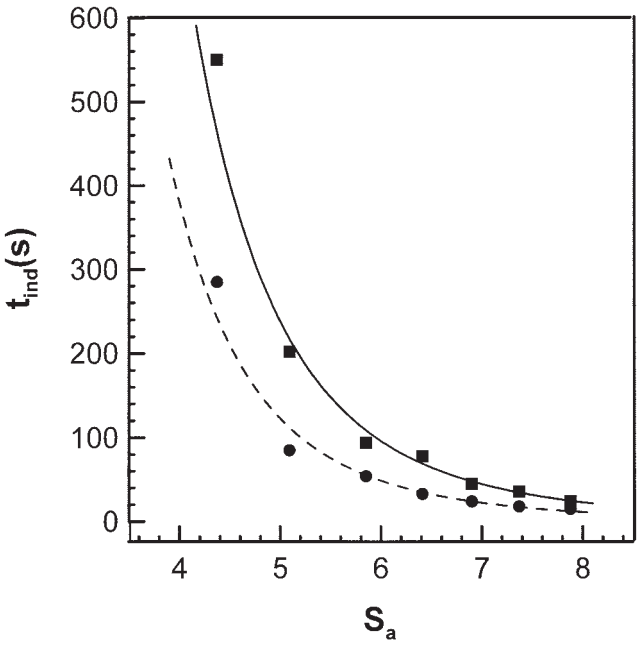

Figure 6. Variation of the induction period as a function of supersaturation at T=298K.

Discrete points represent experimental data and curves represent values predicted by this model. ■ : unseeded case.[24] ● : seeded case.[24] —; unseeded case, model prediction, – – – – ; seeded case, model prediction.

7 into Eq. 4. As can be seen from Figure 5, the performance of this model is satisfactory, except the data at higher ratio of $[Mg^{2+}]/[Ca^{2+}]$ for the case of the lowest initial reagent concentration. This suggests that the presence of Mg^{2+} increases the induction period through raising the interfacial tension and decreasing the association coefficient.

Effect of crystal seeds

The variation of the induction period as a function of supersaturation for the case when crystal seeds are introduced is shown in Figure 6, in which the corresponding results for the case when crystal seeds are absent are also shown for comparison. The curves represent the theoretical value of induction period calculated by Eq. 6a, in which C_o is replaced by C_0'. The concentration of monomers in the vicinity of a seed surface C_0' is evaluated by substituting C_o into Eq. 8. Here, we assume that the association coefficient of clusters is the same as that of the unseeded case, that is, $K_1=2\times10^{-18}$. Figure 6 reveals that the induction period for the seeded case is shorter than that of the unseeded case. The value of ε calculated from the theoretical and experimental values of induction period is 1.05, meaning that the agreement between theoretical values and experimental data is satisfactory. The decrease in the induction period when crystal seeds are present can be explained by an increase in the concentration of clusters near crystal surface. This also implies that van der Waals attractive force between cluster and crystal seed plays a significant role in the formation of critical nuclei of $CaCO_3$ in the secondary nucleation regime. On the basis of atomic force microscopy (AFM) examination on protein, Kuznetsov et al.[25] found that the degree of supersaturation in the vicinity of a crystal is higher than that in the bulk liquid phase. This provides an indirect evidence for this theory.

Conclusion

The effects of supersaturation, temperature, the presence of Mg^{2+} and crystal seeds on the induction period of $CaCO_3$ are studied by employing Smoluchowski's coagulation theory. The analysis of the experimental data reveals that the rate of association between two clusters is independent of their sizes. The association coefficient depends on both the temperature and the presence of impurity. The order of magnitude of the activation energy, which is 200J/mol, suggests that the association between two clusters is of physical nature. The increase in the induction period when Mg^{2+} is present may be caused by an increase in the solid-liquid interfacial energy, and a decrease in the association coefficient between two clusters. The introduction of crystal seeds has the effect of reducing the induction period. This is mainly caused by an increase in the concentration of clusters in the vicinity of seed surface, due to the van der Waals attractive force existing between the clusters and seed crystals.

Acknowledgment

This study is supported by the National Science Council of the Republic of China.

Notation

a_{ij} = the two cluster association coefficient
b_{ij} = the two cluster dissociation coefficient
C_o = initial concentration of solute in the solution, mol/L
C_o' = initial concentration of solute near the surface of seed crystal, mol/L
C_n = the concentration of clusters of size n (n-mer), mol/L
d = distance from the crystal surface, m
E_a = active energy of coagulation, J/mol
g_c = size of critical nuclei
K_1, K_2, K_3 = coagulation rate constant defined in Eqs. 2a, 2b and 2c, L/mol · s
k = Boltzmann constant, J/K
Mw = molecular weight, kg/mol
$\bar{n}$ = the average size of clusters
N = Avogadro number
r_1 = radius of the monomer, m
R = gas constant, J/mol · K
S_a = supersaturation based on activity
t = coagulation time, s
t_{ind} = induction period, s
T = absolute temperature, K
V_m = volume of monomer, m^3
$\gamma_\pm$ = average ionic activity coefficient in the supersaturation solution
ε = total absolute deviation between theoretical and experimental induction periods
ρ = density of crystal, kg/m^3
δ = interfacial energy of the crystal cluster, mJ/m^2

Literature Cited

1. Larson MA, Garside J. Solute clustering in supersaturated solutions. *Chem. Eng. Sci*. 1986;41:1285-1289.
2. Azuma T, Tsukamoto K, Sunagawa I. Clustering phenomenon and growth units in lysozyme aqueous solutions as revealed by Laser light scattering method. *J. Cryst. Growth.* 1989;98:371-376.
3. Myerson AS, Pei YO. Diffusion and cluster formation in supersaturated solutions. *J. Cryst. Growth*. 1990; 99:1048-1052.

4. Söhnel O, Mullin JW. A method for determination of precipitation induction periods. *J. Cryst. Growth*. 1978;44:377-382.
5. Söhnel O, Mullin JW. Precipitation of calcium carbonate. *J. Cryst. Growth*. 1982;60:239-250.
6. Wakita MIH, Masuda I. Analyses of precipitation processes of dis-(Dimethyl- glyoximato)Ni(II) and related complexes. *J. Cryst. Growth*. 1983;61:377-382.
7. Carosso PA, Pelizzetti E. A stopped-flow technique in fast precipitation kinetics-the case of barium sulfate. *J. Cryst. Growth*. 1984;68: 532-536.
8. Kibalczyc W, Bondarczuk K. Light scattering study of calcium phosphate precipitation. *J. Cryst. Growth*. 1985;71:751-756.
9. Glasner A, Tassa M. The thermal effects of nucleation and crystallization of KBr solutions. *J. Cryst. Growth*. 1972;13/14:441-444.
10. Kibalczyc W, Zielenkiewicz A. Calorimetric investigations of calcium phosphate precipitation. *J. Cryst. Growth*. 1987;82:733-736.
11. Verdoes D, Kashchiev D, van Rosmalen GM. Determination of nucleation and growth rates from induction time in seeded and unseeded precipitation of calcium carbonate. *J. Cryst. Growth*. 1982;118:401-413.
12. Gómez-Morales J, Torrent-Burgués J, Rodríguez-Clemente R. Nucleation of calcium carbonate at different initial pH conditions. *J. Cryst. Growth*. 1996;169:331-338.
13. Söhnel O, Mullin JW. Interpretation of crystallization induction periods. *J. Colloid. Interface Sci*. 1988;123:43-50.
14. Qian RY, Botsaris GD. A new mechanism for nuclei formation in suspension crystallizers: the role of interparticle forces. *Chem. Eng. Sci*. 1997;52:3429-3440.
15. Chien WC, Tai CY, Hsu JP. The induction period of the $CaCl_2$-Na_2CO_3 system: theory and experiment. *J. Chem. Phys*. 1999;111: 2657-2664.
16. Cohen RJ, Benedek GB. Equilibrium and kinetic theory of polymerization and the sol-gel transition. *J. Phys. Chem*. 1982;86:3696-3714.
17. Bowen MS, Broide ML, Cohen RJ. Temporal evolution of the cluster size distribution during brownian coagulation. *J. Colloid Interface Sci*. 1985;105:617-627.
18. Mullin JW. *Crystallization*, 3rd ed. Oxford, Butterworth-Heinemann, 1993.
19. Linke, WF. *Solubilities of Inorangic and Metal-Organic Compounds*. New York: Van Nostrand, 1958.
20. Söhnel O, Garside J. *Precipitation: Basic Principles and Industrial Applications*. Oxford: Butterworth-Heinemann, 1992.
21. Bromley LA. Thermodynamic properties of strong electrolytes in aqueous solutions. *AIChE J*. 1973;19:313-320.
22. Tai CY, Chien WC. Interpreting the effects of operating variables on the induction period of $CaCl_2$-Na_2CO_3 system by a cluster coagulation model. *Chem. Eng. Sci.* 2003;58:3233-3241.
23. Bergström L. Hamaker constants of inorganic materials. *Adv. Colloid Interface Sci*. 1997;70:125-169.
24. Tai CY, Chien WC. Effects of operating variables on the induction period of $CaCl_2$-Na_2CO_3 system. *J. Cryst. Growth*. 2002;237/239: 2142-2147.
25. Kuznetsov YG, Malkin AJ, Glantz W, Mcpherson A. *In situ* atomic force microscopy studies of protein and virus crystal growth mechanisms. *J. Cryst. Growth*. 1996;168:63-73.

Manuscript received Nov. 27, 2003, and revision received May 24, 2004.